We are IntechOpen,
the world's leading publisher of
Open Access books
Built by scientists, for scientists

4,800
Open access books available

122,000
International authors and editors

135M
Downloads

Our authors are among the

154
Countries delivered to

TOP 1%
most cited scientists

12.2%
Contributors from top 500 universities

WEB OF SCIENCE™

Selection of our books indexed in the Book Citation Index
in Web of Science™ Core Collection (BKCI)

Interested in publishing with us?
Contact book.department@intechopen.com

Numbers displayed above are based on latest data collected.
For more information visit www.intechopen.com

3

Design Principles of Seismic Isolation

George C. Lee and Zach Liang
Multidisciplinary Center for Earthquake Engineering Research,
University at Buffalo, State University of New York
USA

1. Introduction

In earthquake resistance design of structures, two general concepts have been used. The first is to increase the capacity of the structures to resist the earthquake load effects (mostly horizontal forces) or to increase the dynamic stiffness such as the seismic energy dissipation ability by adding damping systems (both devices and/or structural fuses). The second concept includes seismic isolation systems to reduce the input load effects on structures. Obviously, both concepts can be integrated to achieve an optimal design of earthquake resilient structures. This chapter is focused on the principles of seismic isolation.

It should be pointed out that from the perspective of the structural response control community, earthquake protective systems are generally classified as passive, active and semi-active systems. The passive control area consists of many different categories such as energy dissipation systems, toned-mass systems and vibration isolation systems. This chapter addresses only the passive, seismic isolation systems [Soong and Dargush, 1997; Takewaki, 2009; Liang et al, 2011]

Using seismic isolation devices/systems to control earthquake induced vibration of bridges and buildings is considered to be a relatively matured technology and such devices have been installed in many structures world-wide in recent decades. Design guidelines have been established and they are periodically improved as new information based on research and/or field observations become available during the past 20-30 years [ATC 1995; SEAONC 1986; FEMA 1997; IBC 2000; ECS 2000; AASHTO 2010, ASCE 2007, 2010].

Besides the United States, base isolation technologies are also used in Japan, Italy, New Zealand, China, as well as many other countries and regions. [Naiem and Kelly, 1999; Komodromos, 2000; Christopoulos, C. and Filiatrault 2006]

Affiliated with the increased use of seismic isolation systems, there is an increased demand of various isolation devices manufactured by different vendors. This growth of installing seismic isolation devices in earthquake engineering has been following the typical pattern experienced in structural engineering development, which begins from a "statics" platform by gradually modifying the design approach to include the seismic effects based on structural dynamics principles as they develop and new field observations on the responses of real-world structures. The process is typically slow because most studies and laboratory observations have been concentrated on the performances of the devices with scaled-down experiments. Results could not be readily scaled-up for design purposes. At the same time, there were very limited field data on the actual performances of seismically isolated

structures. In recent years, some limited successful stories were reported in the literature on the seismic performance of base-isolated bridges and buildings during real earthquakes, as well as reports of unsuccessful cases including the failure of isolation bearings and falling spans of bridges and magnification (rather than reduction) of vibration levels of buildings. These structural failures have not been systematically examined for their contributing factors. Some of them include: construction quality, improper choice of the type of isolation bearings, incomplete design principles and methods, unknown ground motion and soil characteristics, etc. In summary, current practice is mainly based on past research and observations on the performance of the isolation devices themselves, with minimum information on the dynamic performance of the structure-device as a system.

The working principle of seismic isolation may be explained in several ways. It is a general understanding that isolation devices/systems are used to reduce the seismic force introduced base shear. Designers often understand the working principles from the viewpoint of design spectrum in that, when the vibration period of a structure is longer than a certain level, continue to increase the period will reduce the magnitude of the spectral value and thus reduce the base shear accordingly. To qualitatively explain the working principle of seismic isolation in this manner is reasonable, but it is insufficient to use it in actual design. Refinements and additional design principles are necessary. Another commonly used explanation of seismic isolation is the "decoupling" of the superstructure vibration from the ground motions excitations to reduce the vibration of structures. This statement again requires quantitative elaborations from the viewpoint of isolation design. In general, an isolation device/system can be viewed as a low-pass mechanical filter of the structure being isolated, to filter out excitations with the undesirable high frequencies to reduce the level of acceleration. In order to establish the cut-off frequency the period of the isolation system must be carefully addressed, and this requires a basic design principle to guide the design.

In order to reduce the base shear, an isolation system must be allowed to deform. This relative displacement cannot be filtered like the absolute acceleration. In general working range, the longer the relative displacement associated with longer periods, the more reduction in base shear can be achieved, except for the fact that the latter will introduce certain negative effects. The most significant issue of large relative displacement is the large P-delta effect and for falling spans in bridges. In this regard, a design principle is needed to achieve the best compromise in seismic isolation design. In reality, the only approach to effectively reduce the relative displacement is to increase damping, which, in turn, will result in higher level of acceleration. This conflicting demand of controlling acceleration and acceptable displacement in essence defines the limiting range of the effectiveness of seismic isolation systems. Quantitatively this issue can be addressed, and this is an important design principle to be conceptually discussed in this chapter.

In Section 2 of this chapter, several important design issues (e.g. P-delta effect, vertical motions, etc.) will be discussed and seismic isolation design principles will be described. In Section 3, the quantitative basis of treating seismically-isolated structures will be briefly reviewed and simplified models will be established for the dynamic analysis and design of the structure-device system. Design methods will be briefly discussed in Section 4, and a newly developed seismic isolation device to address some of the issues facing today's practice is briefly introduced in Section 5. Finally, the key issues and parameters in seismic isolation is summarized and future research needs are briefly noted.

2. Some issues and principles of seismic isolation

In this section, the theories, design and practical considerations of seismic isolation are briefly discussed.

2.1 State-of-practice on seismic isolation
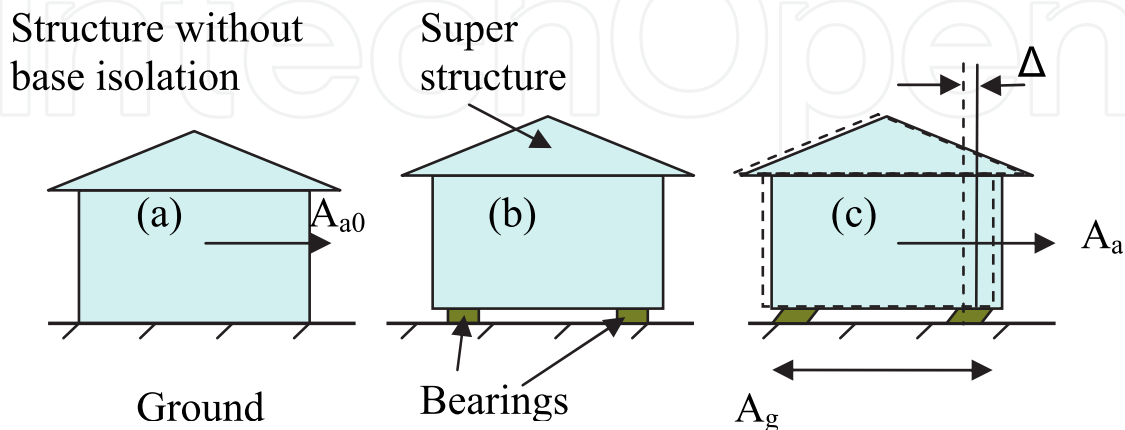The principle of base isolation is typically conceptually explained by using figure 2.1.

Fig. 2.1. Concept of base isolation

Figure 2.1 (a) and (b) show a structure without and with base isolation, respectively. It is seen that the major difference between (a) and (b) is that in (b), the structure is set on top of isolation several bearings. When the ground moves with acceleration A_g, the superstructure will move accordingly with a displacement Δ, and a reduced level of absolute acceleration, denoted by A_a, rather than the original level A_{a0}.

This principle has been the basis for many research and development efforts in design guidelines and devices for seismic isolation. These have been many important contributions during the past 25 years led by Kelly and his associates at Berkeley and Constantinou and his associates at Buffalo as well as many others. (See references listed at the end of this chapter.)

2.2 Basic concept
The major purpose of using the seismic isolation is to reduce the base-shear of the structure. Physically, large base shear is one of the main reasons of structural damages due to strong horizontal ground accelerations. Thus, to reduce the lateral acceleration is a basic principle.

From the viewpoint of design, many aseismic codes use the base shear as a control parameter. For example, if the base shear of a building is reduced, then the upper story lateral forces floor drifts are also reduced. In the case of a bridge, base shear reduction will minimize damage to the piers.

2.2.1 Base shear
Base shear V can be calculated through various approaches. The following are several examples, first

$$V = C_s W \qquad (2.1)$$

where C_s is the seismic response factor and W is the total weight of a structure. Base isolation is intended for reducing C_s, second

$$V = \sum f_{Lj} \quad (kN) \tag{2.2}$$

where f_{Lj} is the later force of the jth story of the structure. Base isolation is intended to reduce f_{Lj} simultaneously, so that the base shear will be reduced, in addition

$$V = K_b \Delta \quad (kN) \tag{2.3}$$

where K_b is the lateral stiffness of the bearing system; Δ is the nominal relative displacement of the bearing. The stiffness K_b of the bearing system will be much smaller than the structure without the bearing, so that the base shear is reduced.

2.2.2 Lateral acceleration

In equation (2.1), C_s is in fact the normalized lateral absolute acceleration A_a, which is in general zero-valued unless earthquake occurs.

$$C_s = A_a / g \tag{2.4}$$

Also note that

$$W = Mg \quad (kN) \tag{2.5}$$

where M is the total mass and $g = 9.8 \ m/s^2$ is the gravity.

In equation (2.2), f_{Lj} is also caused by lateral absolute acceleration a_{aj} of the jth story, that is

$$f_{Lj} = m_j a_{aj} (kN) \tag{2.6}$$

where m_j is the mass of the jth floor.

From (2.5) and (2.6), it is seen that, it is difficult to change or reduce the mass M or m_j in a design; however, if the acceleration can be reduced, the lateral forces will be reduced. Therefore, we will focus the discussion on the acceleration.

2.3 Issues of base isolation

Seismic isolation is considered as a relatively matured technology as evidenced by the many practical applications. These applications have been designed based on codes and provisions that have been established incrementally over time. In the following, seismic isolation principles are examined from a structural dynamics perspective with an objective to suggest additional future research needs.

2.3.1 Absolute acceleration vs. relative displacement

Seen in figure 2.1, to achieve the goal of acceleration reduction, in between the ground and the super structure, there will be installed in a group of bearings, which have much soft stiffness so that the period of the total system will be elongated.

Thus, to achieve acceleration reduction, a major sacrifice is the relative displacement between base and structure must be significantly large. Due to nonlinearities of isolation system, the dynamic displacement can be multiple-centered, which can further notably enlarge the displacement. In addition, permanent residual deformation of bearing may worsen the situation.

Generally speaking, the simplest model of a base isolation system can be expressed as

$$M\, a_a(t) + C\, v(t) + K_b d(t) = 0 \qquad (2.7)$$

where $C\, v(t)$ is the viscous damping force and C is the damping coefficient; $v(t)$ is relative velocity.

In most civil engineering structures, the damping force is very small, that is

$$C\, v(t) \approx 0 \qquad (2.8)$$

Thus, (2.7) can be re-written as

$$M\, A_a \approx K_b \Delta \qquad (2.9)$$

where A_a and Δ are amplitudes of the absolute acceleration $a_a(t)$ and relative displacement $d(t)$. Equation (2.9) describes the relationship between acceleration and displacement of a single-degree-of-freedom (SDOF) system, which can be used to generate the design spectra. Since the damping force is omitted, the generated acceleration is not exactly real, which is referred to as pseudo acceleration, denoted by A_s. Thus, (2.9) is rewritten as

$$M\, A_s = K_b \Delta \qquad (2.10)$$

Furthermore, we have

$$A_s = \omega_b^2\, \Delta \qquad (2.11)$$

where ω_b is the angular natural frequency of the isolation system

$$\omega_b = \sqrt{K_b/M} \ \ (\text{rad/s}) \qquad (2.12)$$

Since the natural period T_b is

$$T_b = 2\,\pi\,/\,\omega_b \ \ (\text{s}) \qquad (2.13)$$

Equation (2.11) can be rewritten as

$$A_s = 4\pi^2/T_b^2\, \Delta \qquad (2.14)$$

From (2.14), the acceleration A_s and displacement Δ are proportional, that is

$$A_s \propto \Delta \qquad (2.15)$$

Since A_s and Δ are deterministic functions, (2.15) indicates that between A_s and Δ, only one parameter is needed, usually, the acceleration is considered.

Combine (2.12), (2.13) and (2.14), it is also seen that A_s is proportional to the stiffness K_b, that is

$$A_s \propto K_b \tag{2.16}$$

That is, the weaker the stiffness is chosen, the smaller value of A_s can be achieved, which is the basis for current design practice of seismic isolation.

From the above discussion, it seems that, as long as K_b is smaller than a certain level, the base isolation would be successful.

However, the above mentioned design principle may have several problems if the assumptions and limitations are not examined. First, from (2.10), it is seen that, only if Δ is fixed, (2.16) holds. On the other hand, if V, that is A_a, is fixed, one can have

$$\Delta \propto 1/K_b \tag{2.17}$$

That is, the weaker the stiffness is chosen, the larger value of Δ can result.

A more accurate model will unveil that, to realize the base isolation, only one parameter, say A_a or Δ, is not sufficient. This is because A_a and Δ are actually independent. In fact, both of them are needed. That is, whenever a claim of the displacement being considered in an isolation design, as long as they are not treated as two independent parameters, the design is questionable. Later, why they must be independent will be explained. Here, let us first use certain group of seismic ground motions as excitations applied on a SDOF system, the ground motion are suggested by Naiem and Kelly (1999) and normalized to have peak ground acceleration (PGA) to be 0.4 (g). The responses are mean plus one standard deviation values, plotted in figure 2.2.
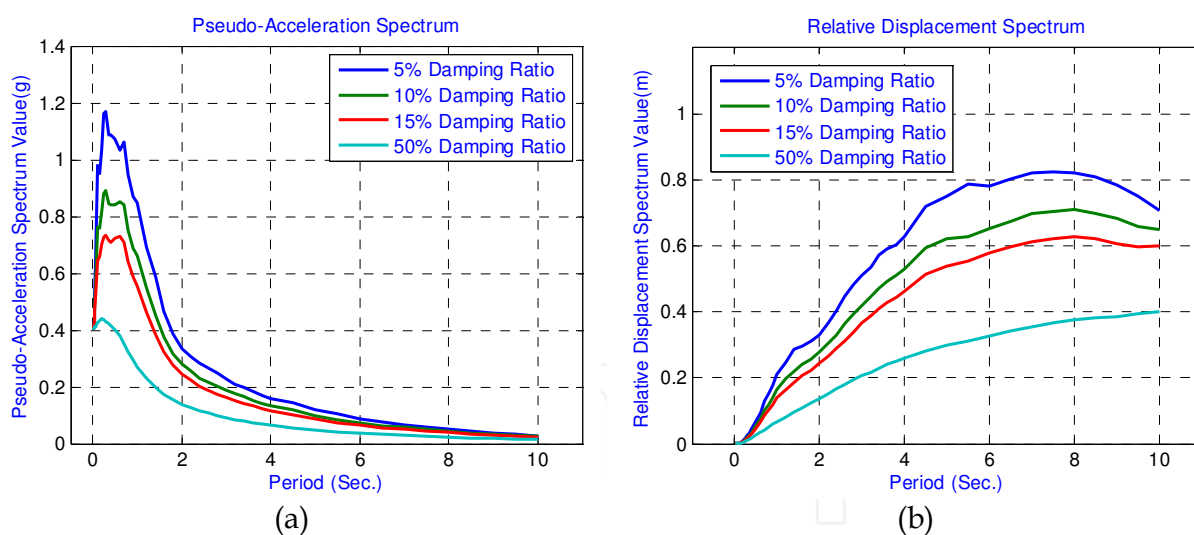

Fig. 2.2. Statistical seismic responses of SDOF systems

Figure 2.2 (a) shows the accelerations of SDOF systems as functions of period for selected damping ratios. When the period becomes larger, the accelerations do reduce, especially when $T_b > 2$ (s). The responses are all smaller than 0.4 (g) and namely, the acceleration is reduced.

Figure 2.2 (b) shows the displacements. It is seen that, when the periods increase, the displacements can become rather large. When $T_b > 2$ (s), the responses can be larger than 0.1 (m), especially if the damping ratio is small, say, 5%.

In figure 2.2 the parameter, damping ratio denoted by ξ is defined by

$$\xi = C / 2\sqrt{MK_b} \tag{2.18}$$

2.3.2 Displacement and center position

Another seismic isolation design issue is the self-centering capacity. Because the SDOF system used to generate the response is linear, and many commercially available bearings are nonlinear systems, the displacement time history can be multiple centered. Figure 2.3 shows examples of a bi-linear (nonlinear) system under Northridge earthquake excitations. The plot in Fig. 2.3 (a) is the displacement time history of the bi-linear system with load and unload stiffness ratio = 0.1 and damping ratio = 0.01. Here the damping ratio is calculated when the system is linear. The plot in Fig 2.3 (b) is the same system with damping ratio = 0.2. It is seen that, the biased deformations exist in both cases. This example illustrates that center shifting can enlarge the displacement significantly, even with heavy damping.

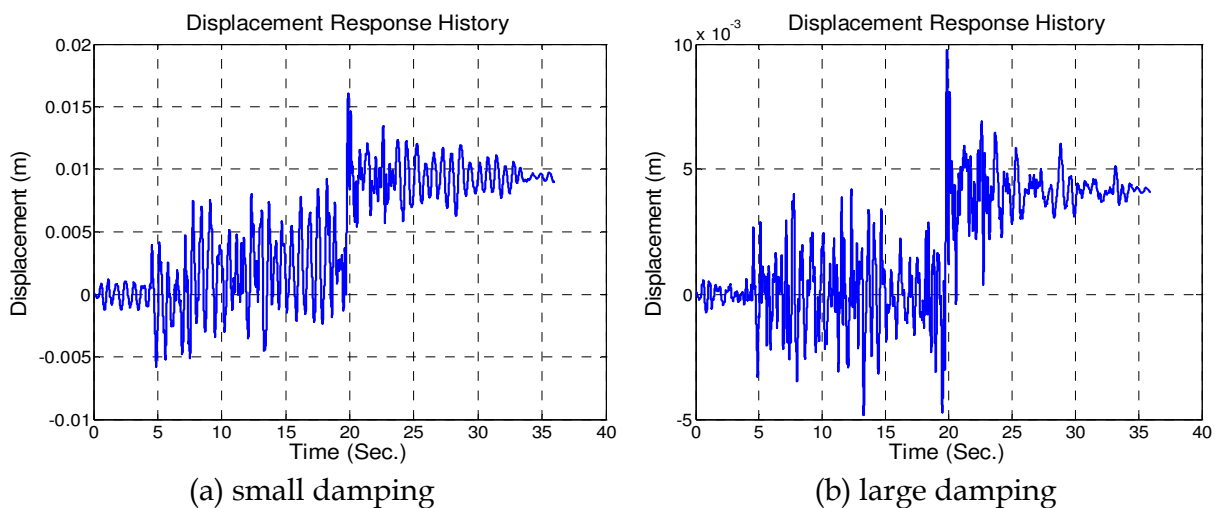(a) small damping   (b) large damping

Fig. 2.3. Multiple centers of displacement responses

Briefly speaking, the current isolation design practice can be based on the spectral analysis, dealing with linear systems with the seismic response coefficient C_s given by

$$C_s = A_s / g = \frac{AS}{T_b B} \tag{2.19}$$

and the spectral displacement d_D given by

$$d_D = D = C_s T_b^2 / 4\pi^2 \, g = \frac{AST_b}{4 \, B} \, (m) \tag{2.20}$$

In the above equations, A is the input level of ground acceleration; S is the site factor; D, instead of Δ, is used to denote the dynamic amplitude and B is called the numerical damping coefficient. Approximately

$$B = 3\xi + 0.9 \tag{2.21}$$

Equations (2.19) and (2.20) will work for most (but not all) situations but cannot handle the position shifting which is a nonlinear response. Some of the nonlinear modeling issues are discussed in Section 3.

2.3.3 SDOF and MDOF models

Many analyses and design of seismic isolations are based on SDOF model, whereas realistic structures are mostly MDOF systems. The acceleration of a higher story of an MDOF system can be much more difficult to reduce.

Equation (2.15) is based on a SDOF system, when the superstructure can be treated as a lumped mass. Namely, the relative deformation among different stories of the structure is negligible. Realistically, such a case is rare; therefore, the acceleration a_{aj} at different stories can be different.

A conventional idea is to decouple a MDOF system into several vibration modes. Each mode is treated as a SDOF system. The total response of the MDOF can then obtained through certain method of modal combinations, such as SRSS method. That is, (2.19) can be rewritten as

$$C_{si} = \frac{AS}{T_{bi}B_i} \tag{2.22}$$

where the subscript i stands for the ith mode. And the ith spectral displacement d_{iD}, (2.20), is rewritten as:

$$d_{iD} = C_{si}\,T_{bi}^2/4\pi^2\;g = \frac{AST_{bi}}{4\,B_i}\;(m) \tag{2.23}$$

where

$$B_i = 3\xi_i + 0.9 \tag{2.24}$$

Furthermore, for multi-story structures, an additional parameter, mode shape, is needed to distribute the acceleration and displacement at different levels. By denoting the mode shape by $\mathbf{P}_i$, which is a vector with the jth element representing the model displacement p_{ji}. The acceleration vector $\mathbf{A}_{si}$ is given as

$$\mathbf{A}_{si} = \Gamma_i C_{si} \mathbf{P}_i\, g = \left\{a_{ji}\right\}\;(m/s^2) \tag{2.25}$$

where a_{ji} is the acceleration of the ith mode at the jth story and Γ_i is the ith modal participation factor.

The displacement vector is given by

$$\mathbf{d}_{si} = \Gamma_i d_{iD} \mathbf{P}_i = \left\{d_{ji}\right\}\;(m) \tag{2.26}$$

where d_{ji} is the displacement of the ith mode at the jth story.

2.3.3.1 Acceleration of higher stories

One of the shortcomings of approximately a MDOF system by a SDOF model is the inability to estimate the responses at the higher levels of a MDOF structure. Typically, through SRSS, the acceleration of the jth story of MDOF system can be calculated as

$$a_{sj} = \sqrt{\sum_i a_{ij}^2} \quad (m/s^2) \tag{2.27}$$

And the displacement of the jth story is

$$d_j = \sqrt{\sum_i d_{ji}^2} \quad (m) \tag{2.28}$$

The reduction of MDOF accelerations is discussed in the literature. The general conclusion is that, (2.25) and (2.27) may not work well so that the acceleration of the higher story a_{sj} may not be calculated correctly. In fact, a_{sj} can be significantly larger.

The reasons of this inaccuracy mainly come from several factors. The first is the damping effect. The second is the error introduced by using only the first mode for design simplicity (the triangular shape function) as illustrated in figure 2.4
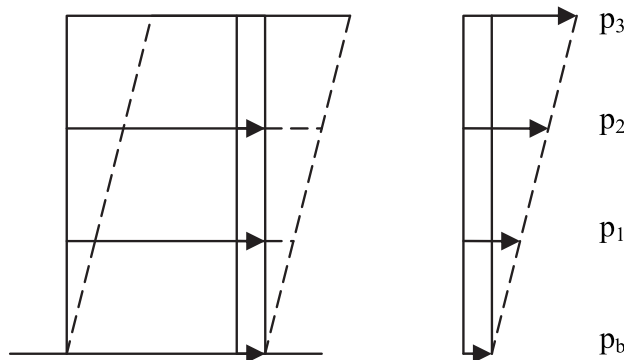

Fig. 2.4. Mode shape function of the 1st mode

In addition, seen from figure 2.4, even through the acceleration of the base, denoted by p_b is rather small by using isolators, the top story will have a rather large acceleration.

2.2.3.2 Cross effects

Another shortcoming of using SDOF models is the inability to estimate the cross effect. Typical MDOF structures have "cross effects" in their dynamic responses. Different from a single member of a structure, which has principal axes, a three-dimensional structure often does not have principal axes. This is conceptually shown in figure 2.5, which is a two story structure. Suppose the first story does have its own principal axes, marked as x_1-y_1, and the second story also has its own principal axes, marked as x_2-y_2. However, from the top view, if x_1 and x_2 are not pointing exactly the same direction, say, there exists an angle θ, then the entire structure will not have principal axes in general. In this case, the inputs from any two perpendicular directions will cause mutual responses. The resulted displacement will be further magnified. This the third reason of large displacement. At present, there are no available methods to quantify cross effects associated with seismic responses, although in general this effect in base isolation design may be small for regularly shaped structures.
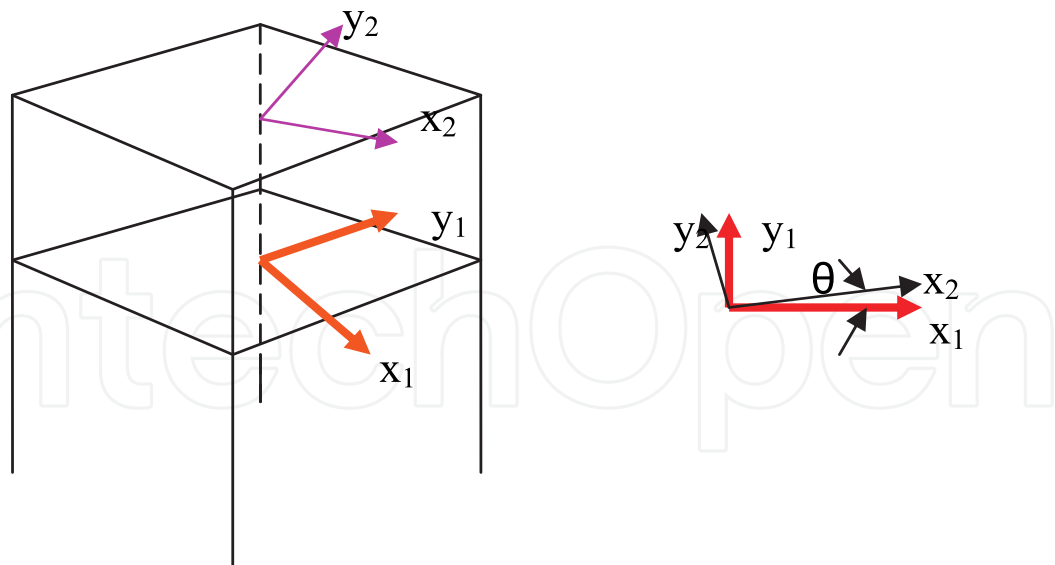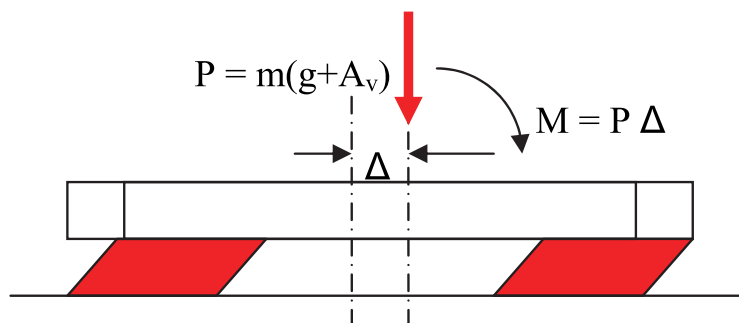
Fig. 2.5. Cross effect

2.3.4 Overturning moment

The product of large vertical load and large bearing displacement forms a large P-Δ effect, conceptually shown in figure 2.6.

Fig. 2.6. Isolation P-Δ effect

This large displacement will result in an overturning moment, given by

$$M = P\Delta = m\left(g + A_v\right)\Delta \tag{2.29}$$

where, the vertical load P is a product of the total weight and the vertical acceleration, the vertical acceleration is the sum of gravity g and earthquake induced acceleration A_v. For example, suppose the total mass is 1000 (ton), the displacement is 0.5 (m), and the additional vertical acceleration is 0.4 (g), the total overturning moment will be 6.86 (MN-m). This is a large magnitude, which requires special consideration in the design of foundations, structure base as well as bearings.

2.3.5 Horizontal and vertical vibrations

As mentioned above, the primary purpose of base isolation is to reduce the horizontal load and/or acceleration. By installing bearings, the lateral stiffness will be significantly reduced so the horizontal vibration can be suppressed. Moreover, by using bearings, the vertical

stiffness can also be reduced to a certain level and the vertical vibration can be magnified. Since the earthquake induced vertical load is often not significantly large, the vertical vibration is often ignored in design. However, due to the magnification of vertical acceleration as well as the above-mentioned large overturning moment, care must be taken to check the vertical load. In the worst scenario, there can be an uplift force acting on bearings with many of them not manufactured to take the uplift load (e.g. rubber bearings).

3. Dynamics of seismically isolated MDOF systems

In this section, base isolation is examined from a different perspective, as a second order mechanical filter of a dynamic system. The working principle of base isolation system is to increase the dynamic stiffness of acceleration without sacrifice too much "dynamic stiffness." Dynamic stiffness is a function of effective period and damping.

3.1 Models of isolation systems
3.1.1 Linear SDOF model
The linear SDOF model is used here to provide a platform to explain the essence of isolation systems under sinusoidal excitation.

A more detailed base isolation model can be rewritten as

$$M\,a(t) + C\,v(t) + K_b d(t) = -M\,a_g(t) \tag{3.1}$$

where a(t) and $a_g(t)$ are respectively the relative and ground accelerations. Note that

$$a_a(t) = a(t) + a_g(t) \tag{3.2}$$

$$a(t) = \dot{v}(t) = \ddot{d}(t) \tag{3.3}$$

where the overhead dot and double dot stand for the first and the second derivatives with respect to time t.

Let the ground displacement $d_g(t)$ be sinusoidal with driving frequency ω_f,

$$d_g(t) = D\cos(\omega_f t) \tag{3.4}$$

The ground acceleration is

$$a_g(t) = A_g\,\cos(\omega_f t) = -D_g\,\omega_f^2\cos(\omega_f t) \tag{3.5}$$

Here, D_g and A_g are respectively the amplitudes of the displacement and acceleration. The amplitude of steady state responses of the relative displacement D can be written as

$$D = \frac{D_g\,\dfrac{\omega_f^2}{\omega_b^2}}{\sqrt{\left(1-\dfrac{\omega_f^2}{\omega_b^2}\right)^2 + \left(2\xi\dfrac{\omega_f}{\omega_b}\right)^2}} = \frac{r^2}{\sqrt{\left(1-r^2\right)^2 + \left(2\xi r\right)^2}}D_g = \beta_d D_g \tag{3.6}$$

Here r is the frequency ratio

$$r = \frac{\omega_f}{\omega_b} \tag{3.7}$$

and β_d is the dynamic magnification factor for the relative displacement

$$\beta_d = \frac{r^2}{\sqrt{\left(1-r^2\right)^2 + \left(2\xi r\right)^2}} \tag{3.8}$$

Note that r = 0 means the driving frequency $\omega_f = 0$ and the system is excited by static force only. In this case, D(r =0) = 0.

The amplitude of steady state responses of the absolute acceleration A_a can be written as

$$A_a = \sqrt{\frac{1+\left(2\xi r\right)^2}{\left(1-r^2\right)^2 + \left(2\xi r\right)^2}} \, A_g = \beta_A A_g \tag{3.9}$$

and β_A is the dynamic magnification factor for the relative displacement

$$\beta_A = \sqrt{\frac{1+\left(2\xi r\right)^2}{\left(1-r^2\right)^2 + \left(2\xi r\right)^2}} \tag{3.10}$$

Note that when the driving frequency $\omega_f = 0$ and the system is excited by static force only. $A_a(r=0) = A_g$. If there exist a static force F_{SA} so that

$$A_g = \frac{F_{SA}}{M} \tag{3.11}$$

Then, when r ≠ 0 or ω_f ≠ 0, the dynamic response of the acceleration can be seen as

$$A_a = \frac{F_{SA}}{M} \beta_A = \frac{F_{SA}}{M/\beta_A} = \frac{F_{SA}}{M_\beta} \tag{3.12}$$

where M_β is called apparent mass or dynamic mass and

$$M_\beta = M/\beta_A \tag{3.13}$$

That is, the value of the dynamic response A_a can be seen as a static force divided by a dynamic mass. From (3.12),

$$M_\beta = \frac{F_{SA}}{A_a} \tag{3.14}$$

The essence described by (3.14) is that the "dynamic mass" equals to a force divided by response. Generally speaking, this term is stiffness. Since the response is dynamic, it can be

called a dynamic stiffness, K_{dA}. In this particular case, the dynamic stiffness is the apparent mass.

$$F_{SA} = K_{dA} A_a \qquad (3.15)$$

Similarly, the relationship between a static force F_{Sd} and a dynamic displacement D can be written as

$$F_{Sd} = K_{dD} D \qquad (3.16)$$

It can be seen that

$$K_{dA} \propto \frac{1}{\beta_A} \qquad (3.17)$$

And

$$K_{dD} \propto \frac{1}{\beta_b} \qquad (3.18)$$

Both the dynamic stiffness and the dynamic factors are functions of frequency ratio r. It can be proven that, the proportional coefficients for (3.17) and (3.18) are constant with respect to r. That is, we can use the plots of dynamic magnification factors to shown the variations of the dynamic stiffness with respect to r. Figure 3.1(a) and (b) show examples of β_A and β_b .

It can be seen from figure 3.1(a), the plot of β_A , when the frequency ratio varies, the amplitude will vary accordingly. Note that,

$$r = \frac{\omega_f}{\omega_b} = \frac{\omega_f}{2\pi} T_b \qquad (3.19)$$

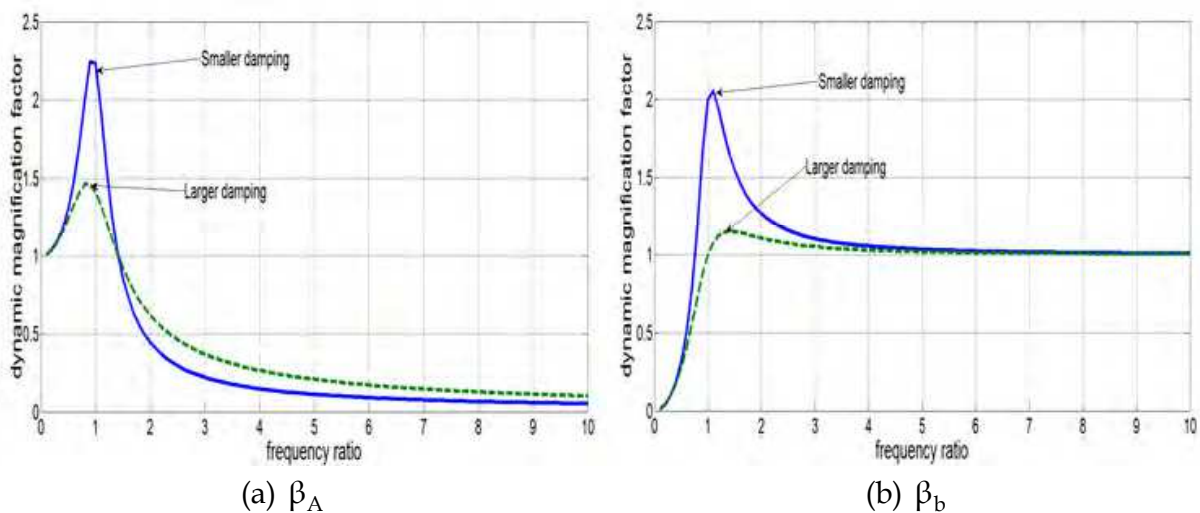(a) β_A (b) β_b

Fig. 3.1. Dynamic magnification factors

That is, if the driving frequency is given, then the frequency ratio r is proportional to the natural period T_b. Therefore, the horizontal plot can be regarded as the varying period. Recall figure 2.2(a) where x-axis is also period. We can realize the similarity of these two plots. First, when the period increases, the amplitudes in both plot increases. After a certain level, these amplitudes start to decrease. It is understandable that, the target of acceleration reduction should be in the region when the accelerations being smaller than a certain level. In figure 3.1 (a), we can clearly realize that this region starts at r = 1.414, which is called *rule 1.4*. To let the isolation system start to work, the natural period should be at least 1.4 times larger than the driving period $T_f = 2\pi/\omega_f$. In the case of earthquake excitation, due to the randomness of ground motions, there is no clear-cut number. However, from figure 2.2 (a), it seems that this number should be even larger than 1.4. In fact, with both numerical simulations and shaking table tests, for linear and nonlinear as well as SDOF and MDOF systems, much higher values of the frequency ratio have been observed by the authors. In general, this limiting ratio should be indeed greater than 1.4.

$$r > 1.4 \qquad\qquad (3.20)$$

Additionally, different damping will result in different response level. In figure 3.1(a), it is seen that, when r > 1.4, larger damping makes the reduction less effective. In figure 2.2 (a), it can be seen that when the period becomes longer, increase damping still further reduce the responses, but the effectiveness is greatly decreased. Note that, this plot is based on statistical results. For many ground excitations, this phenomenon is not always true. That is, increasing damping can indeed reduce the effectiveness of reduction.

Now, consider the displacement. From figure 3.1(b), when the period is near zero, the relative displacement is rather small. Then, as the period increases, the displacement will reach the peak level and then slowly decreases. However, it will never be lower than 1, which means that, the displacement will never below the level of ground displacement.

Increasing the damping, however, will help to reduce the large displacement. This may be seen from Fig. 2.2(b) and it is true for both sinusoidal and earthquake excitations.

3.1.2 Nonlinear SDOF model

The above discussion is based on a linear model. Nonlinear system will have certain differences and can be much more complex to analyze. Generally speaking, many nonlinear systems considerably worsen the problem of large displacement. In the working region, increasing the period will decrease the acceleration but the displacement will remain at a high level. Increasing the damping will help to reduce the displacement but does not help the acceleration.

3.1.2.1 Effective system

It is well understood that, in general, a nonlinear dynamic system does not have a fixed period or damping ratio. However, in most engineering applications, the effective period T_{eff} and damping ratio ξ_{eff} are needed, and are calculated from

$$T_{eff} = \frac{2\pi}{\sqrt{M/K_{eff}}} \qquad\qquad (3.21)$$

And

$$\xi_{eff} = \frac{E_d}{2\pi K_{eff} D^2} \tag{3.22}$$

where E_d is the energy dissipation of the nonlinear system during a full vibration cycle.

From (3.21) and (3.22), it is seen that, to have the effective values, the key issue is to establish the effective stiffness K_{eff}.

In the following, the bi-linear system is used to discuss the effective stiffness, for the sake of simplicity. Although this system is only a portion of the entire nonlinear systems, the basic idea of conservative and dissipative forces seen in the bilinear system can be extended to general nonlinear systems. And, in many cases, nonlinear isolation is indeed modeled as a bi-linear system. Figure 3.2 shows (a) the elastic-perfectly-plastic (EEP) system and (b) the general bi-linear system. Conventionally, the secant 'stiffness" is taken to be the effective stiffness. That is

$$K_{eff} = K_{sec} = \frac{f_N}{D} \tag{3.23}$$

where D is the maximum displacement and f_N is the maximum nonlinear force. In the following, since the system is nonlinear and the .response is random, we use lower case letters to denote the responses in general situations, unless these responses will indeed reach their peak value.
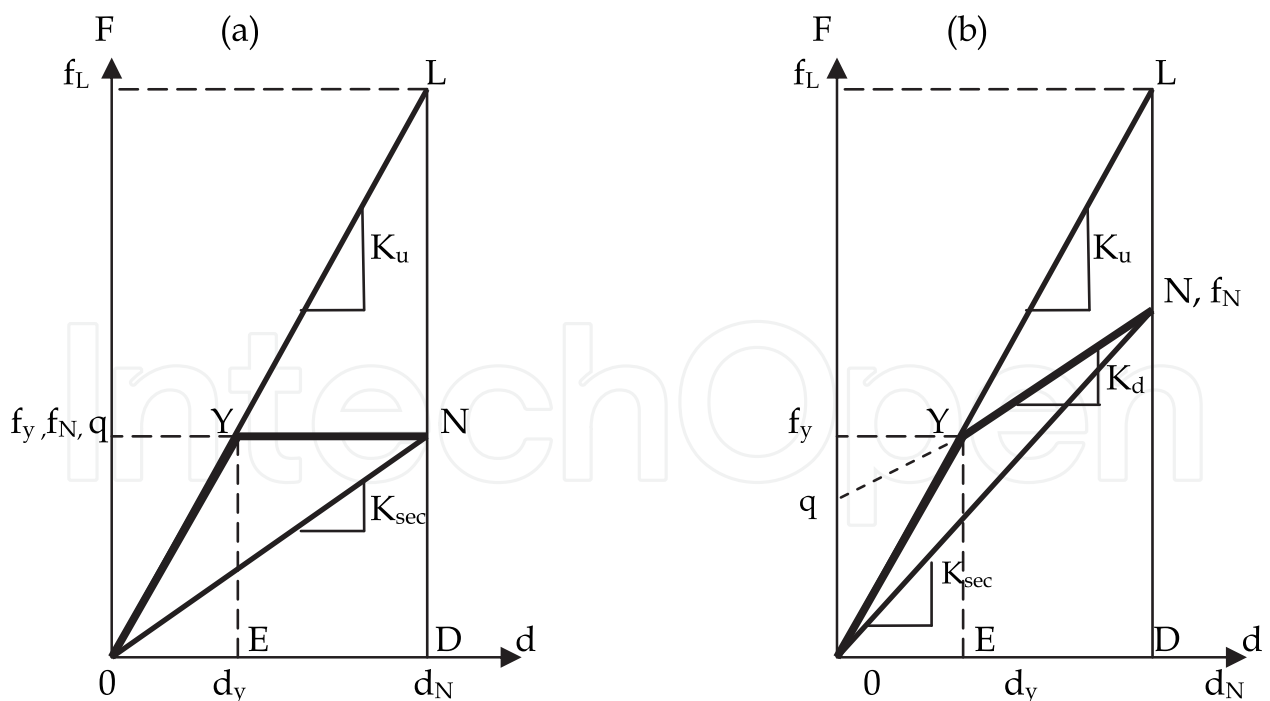

Fig. 3.2. Secant stiffness

In figure 3.2, d_y and d_N are the yielding and the maximum displacements. f_y and f_N are the yielding and the maximum forces. K_d and K_u are the loading and unloading stiffness. If the system remains elastic, then we will have a linear system when the displacement reaches the

maximum value D, the force will be f_L. However, since the system is nonlinear, the maximum force f_N will be smaller. Thus the corresponding effective stiffness will be affected.

For seismic isolation, the measurement of the effective stiffness can be considerably overestimated. To see this point, let us consider the definition of stiffness in a linear system. It is well known that the stiffness denotes capability of how a linear system can resist external force. Suppose under a force f_L, the system has a deformation d, and then the rate defines the stiffness. That is

$$K = \frac{f_L}{D} \tag{3.24}$$

When the load f_L is released, the linear system will return to its original position. Thus, the stiffness also denotes the capacity for how a system can bounce back after the force f_L is removed, for at displacement d, the linear system will have a potential energy E_p

$$E_p = \frac{K\, d^2}{2} \tag{3.25}$$

Therefore, we can have alternate expression for the stiffness, which is

$$K = \frac{2E_p}{d^2} \tag{3.26}$$

Apparently, in a linear system, the above two expressions of the stiffness, described by (3.24) and (3.26), are identical. This is because the potential energy can be written as

$$E_p = \frac{f_L d}{2} \tag{3.27}$$

However, in a nonlinear system, this equation will no longer hold, because the maximum force f_N can contain two components: the dissipative force f_d and the conservative force, f_c,

$$f_N = f_c + f_d \tag{3.28}$$

For example, in Figure 3.2(a), when f_N is reached,

$$f_c = 0$$

$$f_d = q$$

Thus,

$$f_N = f_d = q$$

Namely, the EPP system does not have a conservative force. Its restoring force is zero.

From another example of the general bilinear system shown in figure 3.2 (b),

$$f_d = q$$

and

$$f_c = f_N - f_d$$

Note that, only the conservative force contributes to the potential energy E_p. That is,

$$E_p = \frac{f_c d}{2} < \frac{f_N d}{2} \qquad (3.29)$$

In this case, using (3.24) and (3.26) will contradict each other. In order to choose the right formulae to estimate the effective period and damping, the estimation of effective stiffness must be considered more precisely. Generally speaking, a nonlinear system will have the same problem as the above-mentioned bi-linear system, that is, the restoring force is smaller than the maximum force, as long as the nonlinear system has softening springs.

3.1.2.2 Estimation of effective period

From the above-discussion, when we use an effective linear system to represent a nonlinear system, the effective stiffness should satisfy the following:

$$K_{eff} = \frac{2E_p}{d^2} \qquad (3.30)$$

$$K_{eff} = \frac{f_c}{d} \qquad (3.31)$$

By using (3.30) as well as (3.31), the effective stiffness k_{eff} will be smaller than the secant stiffness k_{sec}.

Furthermore, it can be seen that, vibration is caused by the energy exchange between potential and kinetic energies. The natural frequency of a linear system can be obtained by letting the maximum potential energy equal the maximum kinetic energy, that is, through the relation

$$\frac{k d^2}{2} = \frac{M v^2}{2} = \frac{M \omega_b^2 d^2}{2} \qquad (3.32)$$

In nonlinear systems, we should modify the above equation as

$$\frac{k_{eff} d^2}{2} = \frac{m \omega_{eff}^2 d^2}{2} \qquad (3.33)$$

Or,

$$\omega_{eff} = \sqrt{\frac{k_{eff}}{M}} = \sqrt{\frac{f_c/d}{M}} < \sqrt{\frac{f_N/d}{M}} \qquad (3.34)$$

In other words, considering the dynamic property of a nonlinear system, we should not use the secant stiffness as the effective stiffness. Following this logic, the effective stiffness should be defined in a nonlinear system by considering the restoring potential energy as follows.

In the bi-linear case (see the shaded areas in Figure 3.3), when the system moves from 0 to d, the potential energy is

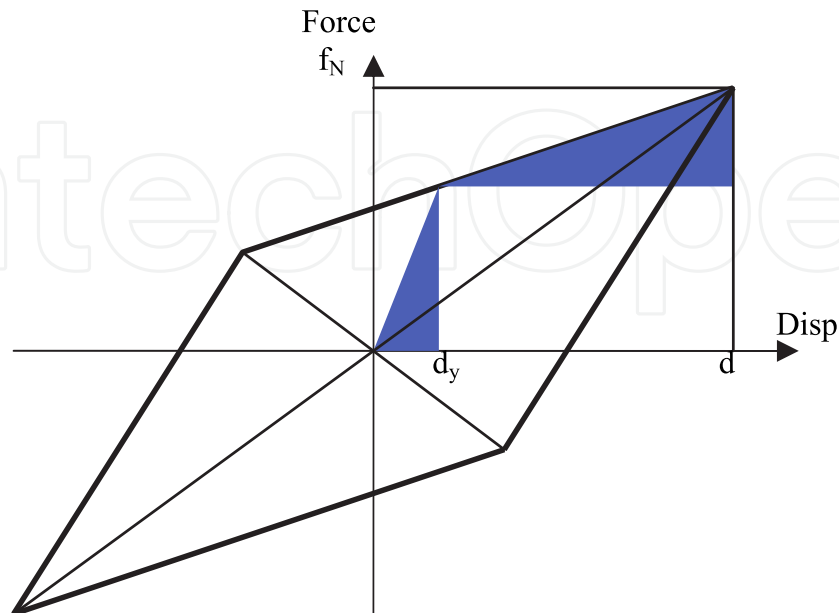$$E_p = \frac{1}{2}\left[K_u d_y^2 + K_d\left(d - d_y\right)^2\right] \tag{3.35}$$

Fig. 3.3. Maximum potential energy of a bi-linear system

Therefore,

$$K_{eff} = \frac{2E_p}{d^2} = \frac{K_u d_y^2 + K_d\left(d - d_y\right)^2}{d^2} \tag{3.36}$$

By using the displacement ductility μ, we can write

$$K_{eff} = \frac{K_u + K_d\left(\mu - 1\right)^2}{\mu^2} \tag{3.37}$$

where μ is the displacement ductility and

$$\mu = \frac{d}{d_y} \tag{3.38}$$

The relationship between K_d and K_u is given as

$$K_d = a\, K_u \tag{3.39}$$

Using this notation, we have

$$K_{eff} = \frac{1 + a\left(\mu - 1\right)^2}{\mu^2} K_u \tag{3.40}$$

Therefore, the corresponding effective period is

$$T_{eff} = \sqrt{\frac{\mu^2}{1 + a(\mu - 1)^2}} \; T_1 = 2\pi \, \mu \sqrt{\frac{M}{\left[1 + a(\mu - 1)^2\right] K_u}} \qquad (3.41)$$

From (3.41) and (3.23), the effective stiffness estimated by the secant method can overestimate the period by the factor

$$\frac{\dfrac{1 + a(\mu - 1)}{\mu}}{\dfrac{1 + a(\mu - 1)^2}{\mu^2}} = \frac{1 + a(\mu - 1)}{1 + a(\mu - 1)^2} \mu \qquad (3.42)$$

Note that, the term a is smaller than unity and μ is larger than unity. Therefore, from (3.42), it is seen that the period can be notably underestimated by using the secant stiffness. For example, suppose a = 0.2 and μ = 4, the factor will be greater than 2.

Similar to the estimation of effective period, the term K_{eff} will also affect the measurement of the effective damping ratio. Using the same logic, the damping ratio can also be underestimated. These double underestimations may cancel each other to a certain degree for acceleration computation, but will certainly underestimate the displacement. For a detailed discussion on structural damping, reference is made to Liang et al (2012).

3.1.3 MDOF models

Now, let use consider a linear n-DOF systems along one direction, say the X-direction. The governing equation can be written as

$$\mathbf{M}\ddot{X}(t) + \mathbf{C}\dot{X}(t) + \mathbf{K}X(t) = -\mathbf{M}\,J\,a_g(t) \qquad (3.43)$$

Here **M**, **C** and **K** are nxn mass, damping and stiffness matrices, $J = \{1\}_{nx1}$ is the input column vector and

$$X(t) = \begin{Bmatrix} d_1(t) \\ d_2(t) \\ \dots \\ d_n(t) \end{Bmatrix}_{nx1} \qquad (3.44)$$

where $d_j(t)$ is the displacement at the jth location.

If the following Caughey criterion hold

$$\mathbf{C}\mathbf{M}^{-1}\,\mathbf{K} = \mathbf{K}\,\mathbf{M}^{-1}\,\mathbf{C} \qquad (3.45)$$

The system is proportionally damped, which can be decoupled into n-SDOF systems, which are referred to as n-normal modes, so that the analysis of SDOF system can be used.

In base isolation, to regulate the displacement, large damping must be used. When the damping force is larger, isolation system is often not proportionally damped. That is, (3.45) will no longer hold and the system cannot be decoupled into n SDOF normal modes. In this case, it should be decoupled in 2n state space by using the state equations.

Configuration of MDOF structures and non-proportional damping will both affect the magnitude of the accelerations of higher stories. However, the acceleration of the base, as well as the relative displacement between the base and the ground will not be significantly affected by using the normal mode approach. Practically speaking, more accurately estimate the displacement is important then the computation of the acceleration of higher stories.

Furthermore, when the isolation system is non-linear, its first "effective" mode will dominate. Thus, we can use its first "effective" mode only to design the system.

However, care must be taken when the cross effect occurs. It is seen that, if both the motion of both X and Y directions, which are perpendicular, are considered, we can have

$$\begin{bmatrix} \mathbf{M}_X & \\ & \mathbf{M}_Y \end{bmatrix} \begin{Bmatrix} \ddot{X} \\ \ddot{Y} \end{Bmatrix} + \begin{bmatrix} \mathbf{C}_{XX} & \mathbf{C}_{XY} \\ \mathbf{C}_{YX} & \mathbf{C}_{YY} \end{bmatrix} \begin{Bmatrix} \dot{X} \\ \dot{Y} \end{Bmatrix} + \begin{bmatrix} \mathbf{K}_{XX} & \mathbf{K}_{XY} \\ \mathbf{K}_{YX} & \mathbf{K}_{YY} \end{bmatrix} \begin{Bmatrix} X \\ Y \end{Bmatrix} = \begin{bmatrix} \mathbf{M}_X & \\ & \mathbf{M}_Y \end{bmatrix} \begin{Bmatrix} J\, a_{xg} \\ J\, a_{yg} \end{Bmatrix} \tag{3.46}$$

where a_{xg} and a_{yg} are ground accelerations along X and Y directions respectively, which are time variables and for the sake of simplicity, we omit the symbol (t) in equation (3.46). The subscript X and Y denote the directions. The subscript XX means the input is in x direction and the response is also in X direction. The subscript XY means the input is in X direction and the response is in Y direction, and so on.

In (3.46), $\mathbf{M}_X = \mathbf{M}_Y$ are the mass matrices. It is seen that, both $\mathbf{C}_{XY} = \mathbf{C}_{YX}{}^T$ and $\mathbf{K}_{XY} = \mathbf{K}_{YX}{}^T$ are the cross terms. Generally speaking, if the system is rotated with the help of rotation matrix we can minimize the cross terms $\mathbf{C}_{XY}$ and $\mathbf{K}_{XY}$.

$$\Theta = \begin{bmatrix} \cos(\theta)\mathbf{I} & -\sin(\theta)\mathbf{I} \\ \sin(\theta)\mathbf{I} & \cos(\theta)\mathbf{I} \end{bmatrix}_{2n \times 2n} \tag{3.47}$$

The angle θ can be chosen from 0 to 90^0. However, in this case no matter how the angle θ is chosen, at least one of $\mathbf{C}_{XY}$ and $\mathbf{K}_{XY}$ is not null and hence, the input in X direction will cause the response in Y direction. That is defined here as the *cross effect*, which implies energies of ground motions from one direction is transferred to another. There are many reasons to generate the cross effect. In certain cases, the cross effect can considerably magnify the displacement.

3.2 Bearings and effect of damping
3.2.1 Role of damping

From the above discussion, it is seen that there are several possible inaccuracies that may exist in estimating the displacement. The results can often be underestimation of displacement in isolation design.

As pointed out earlier, the only way to reduce the displacement in the working range of isolation systems is to increase the damping. For example, from figure 2.2(b), it is seen that, at 3 second period, if the damping ratio is taken to be 50%, the displacement is about 0.2 (m) whereas using 5% only can cause about 0.5 (m) displacement, which is about 2.5 times larger.

3.2.2 Damping and restoring stiffness

Often base isolators or isolation bearings are designed to provide the required damping. Practically speaking, damping can be generated by several means.

The first kind of damping is material damping, such as high damping rubber bearings, lead-core rubber bearings as well as metallic dampers. The damping mechanism is generated through material deformations. Note that, high damping rubbers often do not provide sufficient damping.

The second is surface damping. The damping mechanism is generated through surface frictions of two moving parts, such as pendulum bearings, friction dampers. Note that, surface damping often is insufficient and can have a significant variation from time to time.

The third type of damping is viscous damping, which is often provided by hydraulic dampers. This kind of damping is more stable but with higher cost.

Closely related to damping generated by isolator is the restoring stiffness, since both of them are provided by bearings. In fact, the type of method of proving restoring stiffness and damping classifies the type of bearings.

The restoring stiffness can be generated by material deformations, including specific springs, which relies on the deformation to restore potential energy. Releasing of such potential energy can make the bearing return to its center position. Rubber bearings, including high damping rubber bearings, lead core rubbers bearings, steel-rubber-layered bearings fall into this category. Bearings with sliding surface and elastomeric springs also use restoring force generated by material deformation. Bearings with metal ribs which provide both stiffness and damping also fall into this category.

The restoring stiffness can also be generated by geometric shaped. Generally, when horizontal motion occurs, such bearings generate vertical movement which can also restore potential energy. Again, release of potential energy enables the bearing return to its center position. Pendulum sliding bearing falls into this category. Recently, a newly type of roller bearing is developed, which guarantees a low level constant horizontal acceleration, and will be described in Section 5.

4. Selected design considerations

4.1 Design windows

As mentioned earlier, the key issue in design of isolation system is an optimal compromise of the acceleration and the displacement, within an acceptable range of the period called "design window" period. The reason to consider the concept of design window is to avoid possible undesired displacement, which in general is independent to acceleration.

4.1.1 Lower bond of period

In order to reduce the acceleration, the period of the isolation system cannot be shorter than a given value. Although this value depends upon the site, it can be roughly estimated to be 1.5 to 2 seconds. This value actually establishes the left boundary of the design windows on the design spectrum. This lower limit is well understood. Because of the assumption of negligible damping, acceleration is taking as directly proportional to the displacement. Thus in typical design practice, it is assumed that displacement bound is given once the acceleration limit is established. This is not always true, because acceleration and displacement are in general independent.

4.1.2 Upper bond of period

In order to limit the displacement to a reasonable value, the period of the isolation system cannot be too long. This defines the right side boundary of the design window. In figure 4.1, the design spectrum and the design window for the isolation system is conceptually illustrated.
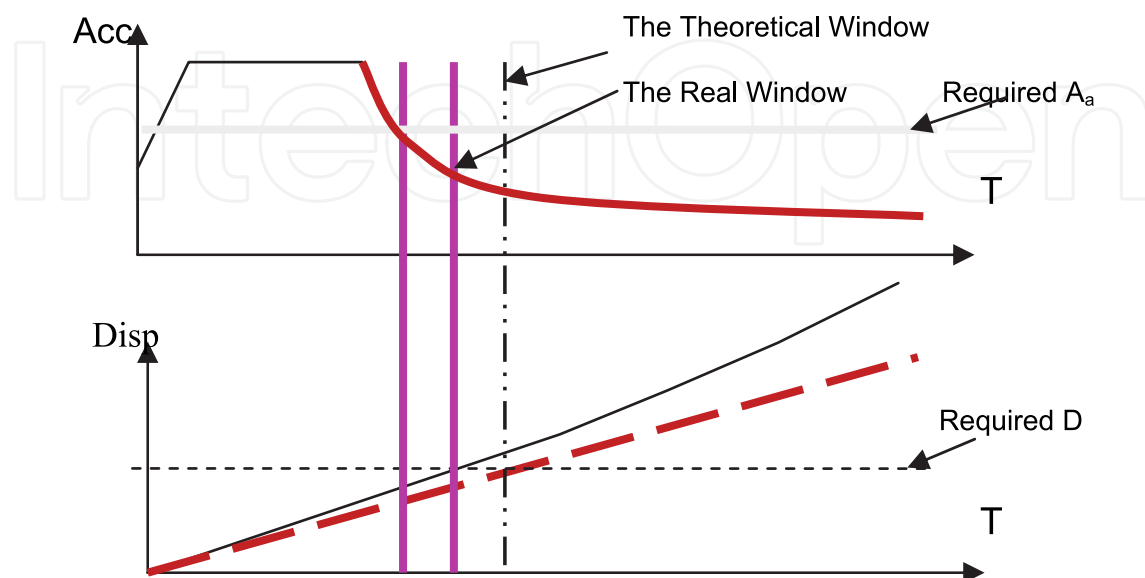

Fig. 4.1. Design Window for Isolation Systems

Figure 4.1 illustrates that if the design has a period that falls outside this "window," it is unacceptable. Within this window, reductions of the acceleration and tolerance displacement must be considered simultaneously. In this sense, a proper isolation system is an optimally compromised design.

It should be noted that, when damping is large, the reduction of acceleration will be reduced. When damping is too low, the displacement will be increased. Thus, the proper damping will have upper and lower period bonds from the viewpoint of isolation design.

4.2 Left boundary of the design window, acceleration related parameters
4.2.1 Design force

In a typical aseismic design, the base shear V typically needs to be designed by

$$s_A V \leq [V] \tag{4.1}$$

where [V] is the allowable base shear and s_A is a factor of safety. The base shear V can be determined by several ways. One is that given by (2.1), which is repeated here.

$$V = C_s W \tag{4.2}$$

To determine the seismic response factor C_s, the effective stiffness K_{eff}, or K_{eff} in the case of MDOF system is required. The effective stiffness often should not be determined by using the secant stiffness, as previously explained.

At the same time, the base shear is equal to the product of the lateral stiffness K_b and the displacement D of the bearing system plus the damping force F_d measured at the maximum displacement.

$$V = K_b D + F_d \qquad (4.3)$$

The specifications related to the damping force for isolators are provided by bearing vendors. For bi-linear damping, the damping force is roughly the dissipative force or the characteristic strength q (see fig. 3.2b). Using the maximum value of q, denoted by Q,

$$F_d = Q \qquad (4.4)$$

For friction damping

$$F_d = \mu W \qquad (4.5)$$

where μ is the friction coefficient.

For multi-story structures, base on the SRSS method,

$$V = \sqrt{\sum_{j=1}^{n} f_{Lj}^2} \qquad (4.6)$$

where, f_{Lj} is the lateral force of the jth story and

$$f_{Lj} = m_j \sqrt{\sum_{i=1}^{S} a_{ji}^2} \qquad (4.7)$$

in which m_j is the mass of the jth story and a_{ji} is the absolute acceleration of the ith mode at the jth story. Note that, for an n-DOF system, there will be n- modal accelerations, and, usually the first few modes will contain sufficient vibration energy of the system. To be on the safe side, the desirable number of modes to be considered is

$$S = S_r + S_f \qquad (4.8)$$

where S_r is the number of the first few modes that contain 90~95% vibration energy and

$$S_f = 1\text{~}3, \qquad (4.9)$$

as an extra safety margin particularly for irregular structures. This should not add too much computational burden.

To determine S_r, modal mass ratio γ_i is often needed,

$$\gamma_i = \frac{\left(\mathbf{P}_i^{\mathrm{T}} \mathbf{M} \, \mathrm{J}\right)^2}{\mathbf{P}_i^{\mathrm{T}} \mathbf{M} \, \mathbf{P}_i} \qquad (4.10)$$

and S_r can be determined by

$$\sum_{i=1}^{S_r} \gamma_i > 90\text{~}95\% \qquad (4.11)$$

In (4.7) the absolute acceleration a_{ji} is the jth element of the ith acceleration vector $\mathbf{a}_i$, which is determined by

$$\mathbf{a}_i = \Gamma_i\, C_{si}\, \mathbf{P}_i \tag{4.12}$$

The term C_{si} is the ith seismic coefficient, which can be determined through the building or bridge code. The modal participation factor Γ_i is given by

$$\Gamma_i = \frac{\mathbf{P}_i^{\mathrm{T}} \mathbf{M}\, \mathbf{J}}{\mathbf{P}_i^{\mathrm{T}} \mathbf{M}\, \mathbf{P}_i} \tag{4.13}$$

Equations (4.10), (4.12) and (4.13) contain the mode shape function $\mathbf{P}_i$ which can be a triangular approximation, or more precisely, be given by the following eigen-equation with the normalization by letting the roof modal displacement equal to unity.

$$\omega_i^2\, \mathbf{P}_i = (\mathbf{M}^{-1}\mathbf{K})\, \mathbf{P}_i \tag{4.14}$$

Note that, the base shear calculated from (4.2) only considers the first mode, which may not be sufficiently accurate. Equation (4.3), is theoretically workable but practically speaking, the dissipative force F_d is difficult to establish.

Note that, in (4.12), the mode shape $\mathbf{P}_i$ is obtained through (4.14), however, $\mathbf{P}_i$ is the displacement mode shape but not necessarily the acceleration mode shape. Therefore, cares must be taken by using (4.12) to calculate the modal acceleration; otherwise a design error can be introduced. For the limited space, the detailed explanation is not discussed in this chapter. Interested reader may see Liang et al 2012.

4.2.2 Overturning moment

Because of the potentially large P-Δ effect, base isolation design must carefully consider the overturning moment to ensure that the uplifting force is not magnified. Furthermore, most bearings cannot take tensions, whereas the overturning moment can generate uplift tension on bearings.
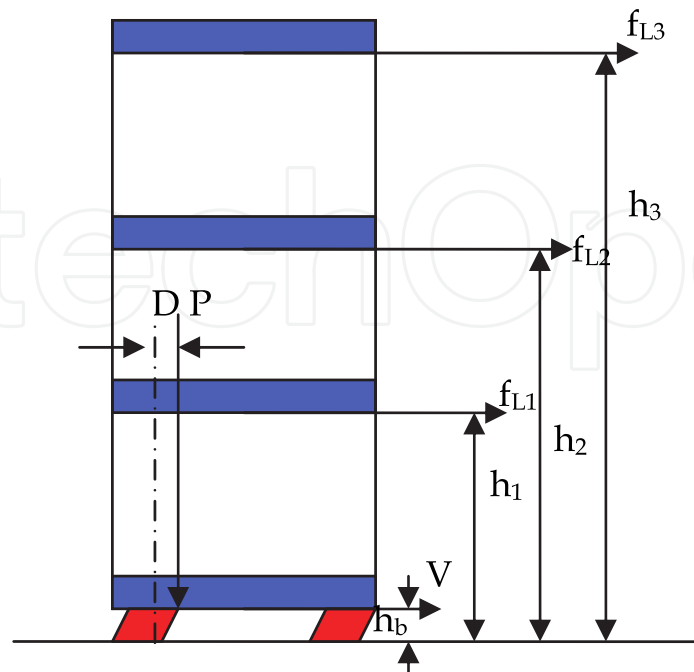

Fig. 4.2. Overturning moment

From figure 4.2, it is seen that the total overturning moment is given by

$$M_T = P D + V h_b + \sum_{j=1}^{n} f_{Lj} h_j \tag{4.15}$$

If the structure has notable plan irregularity, the additional moment due to the asymmetric distribution of mass must also be considered.
With the help of M_T and knowing the geometric dimensions of the isolated structure, the uplift force can be calculated, and the corresponding criterion can be set up as

$$s_M M_T \leq [M_T] \tag{4.16}$$

where s_M is a safety factor and $[M_T]$ is allowable moment.
The above two criteria define the left side boundary of the design window (see fig 4.1).

4.3 Right boundary of design window: Independency of displacement
4.3.1 Independency of displacement
That the displacement D and the acceleration A_a are independent parameters mentioned previously will be briefly explained here. For linear system, from (2.7) we have

$$d(t) = -\frac{C}{K_b} v(t) - \frac{M}{K_b} a_a(t) \tag{4.17}$$

For large amount of damping, consider the peak values, we have

$$D \approx \sqrt{\left(\frac{C}{K_b} V\right)^2 + \left(\frac{M}{K_b} A_a\right)^2} > \frac{M}{K_b} A_a = \omega_b^2 A_a \tag{4.18}$$

Additionally, for nonlinear system, softening behavior often occurs, so that the maximum force is not proportional to the maximum displacement. As a result, one cannot simply calculate D due to the nonlinearity of the most isolation systems, as

$$D = \frac{T_b^2}{4\pi^2} C_s \, g \tag{4.19}$$

In design, the bearing displacement is as important as the acceleration related parameters. Due to the uncertainties illustrated above, a safety factor should be used before further research results are available.

$$s_D D \leq [D] \tag{4.20}$$

where s_D is a safety factor and $[D]$ is allowable displacement.

4.3.2 Right boundary due to displacement
Since the displacement needs to be regulated, the right boundary of the design window is defined. Because of the above-mentioned reasons, by using the safety factor s_D, the right boundary will further shift leftwards.

It is seen that, the resulted window can be rather narrow.

4.4 Probability-base isolation design

In recent years, the probability-based design for civil engineering structures against natural and man-made load effects attracts more and more attentions. The basic idea is to treat both the loads and resistance of structures as random variables and to calculate the corresponding failure probability, based on which the load and resistant factors are specified, (see Nowak and Collins, 2000). Probability-based design for base isolation systems should be one of the frontier research areas for earthquake engineering researchers.

4.4.1 Failure probabilities of base-isolated structures

In the above discussions of seismic isolation, the design process is a deterministic approach because it is established on deterministic data.

A base-isolated building or bridge is a combination of civil engineering structures and mechanical devices, the bearings. In most cases of mechanical engineering devices, the safety factors are considerably larger than those used by civil engineers. The main reason, among many, is that the civil engineering structures have much larger redundancy. Mechanical devices, on the other hand, do not have such a safety margin. This raises an interesting issue on safety factors for seismically isolated structures.

Take the well known design spectrum, for example. Its spectral value is often generated by the sum of mean value plus one standard deviation. However, the maximum value can be much larger than the spectral value. For example, consider under 99 earthquake statistics of a structure with period = 2 second and damping ratio = 20%. The mean-plus-one standard deviation value of acceleration is 0.24 (g) whereas the maximum value is 0.47 (g). And the mean-plus-one standard deviation value of displacement is 0.22 (m), whereas the maximum displacement value is 0.45(m).

The question is: Given an isolation design, what is the chance that 0.47 (g) acceleration and/or 0.45 (m) displacement could occur? More specifically, if the allowed acceleration [A] and/or the allowed displacement [D] are preset, what is the chance that the acceleration and/or the bearing displacement can exceed the allowed design values? From the viewpoint of probability based design, the above-mentioned chance of exceeding is referred to as the failure probability. Therefore, a new concept of design criteria for seismic isolation may be stated by

$$p_{fA} = P(A \geq [A]) \leq [p_{fA}] \tag{4.21}$$

and

$$p_{fD} = P(D \geq [D]) \leq [p_{AD}] \tag{4.22}$$

Here, the subscripts f_A and f_D stand for failure of acceleration and failure of displacement respectively. Symbol [(.)] means the allowable value of (.).

4.4.2 Computation of failure probabilities

Figure 4.3 illustrates the probability distributions of a linear isolation system of $T_b = 2$ second and $\xi = 20\%$ under the excitation of 99 earthquake records. Figure 4.3(a) is the absolute acceleration and (b) is the relative displacement. The X-axes are the numerically

simulated values. The y axes are the probability density function. For example, in figure 4.3(a), this function is denoted as $f_A(a)$, namely the probability density curve is a function of the level of acceleration a.

Suppose the allowed acceleration

$$[A] = 0.25 \text{ (g)}$$

The failure probability can be calculated as

$$p_{fA} = \int_{0.25}^{\infty} f_A(a) \, \mathrm{d}a$$

The integral is the shadow area. From figure 4.3 (a), we can see that, it is about 16%. This failure probability is not small at all. Note that, in this case, the allowed value being 0.25 (g) is satisfied by using the mean-plus-one-standard-deviation value.

As another example, suppose the allowed displacement is

$$[D] = 0.29 \text{ (m)}$$

(a)   (b)
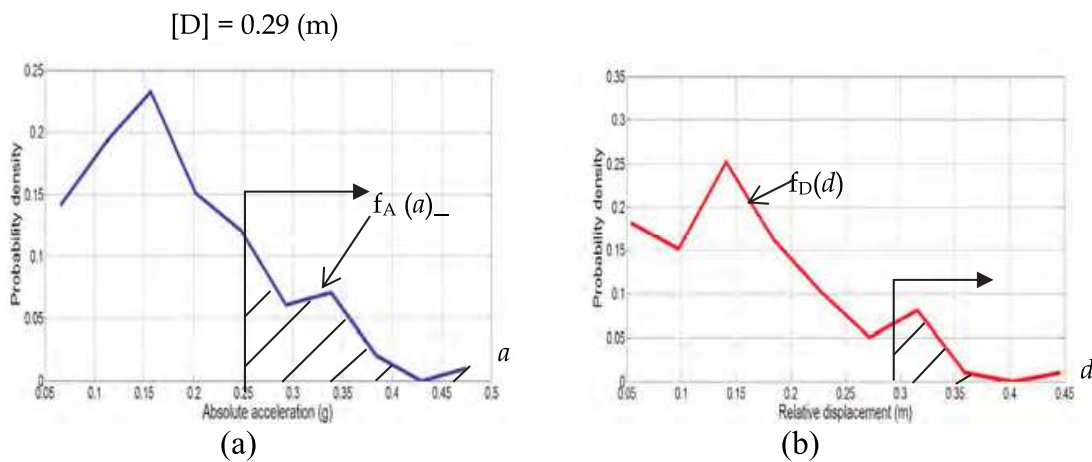
Fig. 4.3. Probability distributions, $T_b = 2$ (sec), $\xi = 20\%$, 99 records, PGA = 0.4 (g).

The failure probability can be calculated as

$$p_{fD} = \int_{0.29}^{\infty} f_D(d) \, \mathrm{d}d$$

The integral is also the shadow area. From figure 4.3 (b), we can also see that, this failure probability is not small either. Note that, in this case, the allowed value being 0.29 (m) is satisfied by using the mean-pulse-one-standard-deviation value.

Generally, the computations can be described as follows

$$p_{fA} = \int_{[A]}^{\infty} f_A(a) \, \mathrm{d}a \qquad (4.23)$$

for acceleration and

$$p_{fD} = \int_{[D]}^{\infty} f_D(d) \, \mathrm{d}d \qquad (4.24)$$

for displacement.

The failure probability implies the chance of not meeting the design requirement. For acceleration, because of the structural redundancy of earthquake resilience, the allowed failure probability can be higher. Anyhow, 15% chance of failure may not acceptable by the owners of the structures (e.g. seismic isolation systems for nuclear reactors). For displacement, usually a bearing cannot tolerance virtually any exceedance. Thus, the allowed failure probability should also be lower.

This brief discussion above suggests that the design safety considerations for the combined civil engineering structures with mechanical devices may be examined by using a probability-based principle and approach.

4.5 Seismic isolation bearings

There are several types of isolation bearings commercially available, such as lead-rubber, high damping rubber as well as sliding bearings. Generally speaking, as long as the bearing system can satisfy the requirement of the above-mentioned design windows in the service life time of the isolation system, any bearing may be employed. Interested readers can consult Komodromos, P.I. (2000). In seismic isolation design, it is suggested that the allowed bearing displacement be used as the primary criterion; the effective period obtained via effective stiffness as the second criterion and providing the proper amount of damping as the third criterion for bearing selections. Because of the difficulty to choose correct type of bearings within the design window, a new type of bearing is introduced as described in Section 5. .

In the literature, certain non-traditional approaches of using relatively inexpensive bearings are reported. Many inexpensive bearings do not allow large displacements and have very limited service life. Therefore, they should not play an important role in seismic isolation design for bridges. Furthermore, the cost of the isolation bearing is often a smaller fraction of the total cost of bridge construction. In most cases, using inexpensive bearings may not be a good choice.

5. A new seismic isolation device

The above discussion on seismic isolation technology suggests that there are many aspects which require further research and development efforts, especially in the area to establish quantitative boundaries of design period in order to achieve optimal designs. In fact, among all commercially available base isolators, none seems to provide a good balance between acceleration reduction and reasonable cost. A recent development, the roller bearing, is briefly explained in this section. It has the promise to utilize damping to achieve desirable compromise in isolative design.

5.1 Concept of roller bearing

The core component of this device is the rolling assembly, which generates a desired low and constant acceleration of the superstructure regardless of the magnitude of the ground excitations. To explain the principle of constant acceleration, consider the simplified sketch of a roller traveling on an inclined surface shown in figure 5.1.

In figure 5.1, the inclined surface shown has a constant slope with an angle θ measured from the horizontal axis. The motion has an absolute acceleration in the horizontal direction, denoted by a_h. The roller has a relative acceleration a_r along the sloping surface, which has a

vertical component a_v and a horizontal component a_{rh}. A_g is the ground acceleration which is acting in the horizontal direction without a vertical component: In other words, the roller will have an absolute vertical acceleration, which is a_v.
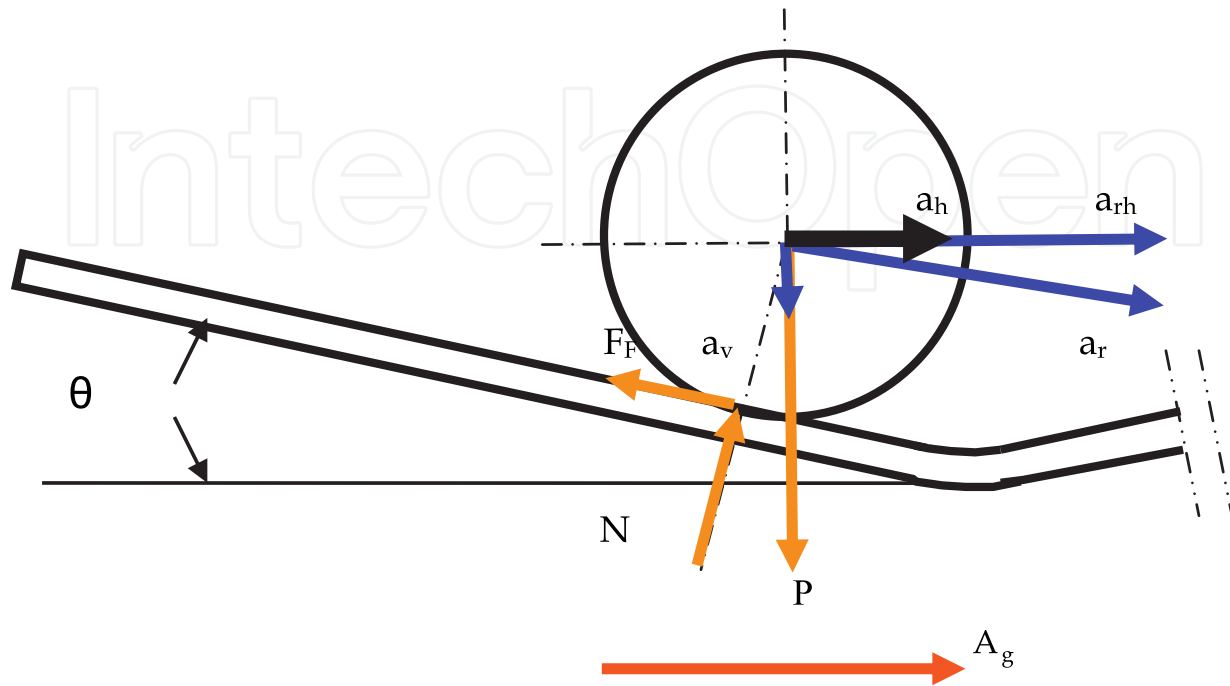

Fig. 5.1. Accelerations and forces of roller bearing

From figure 5.1, it is seen that, the amplitude of the friction force is

$$F_F = \mu N \qquad (5.1)$$

where μ is the rolling friction coefficient.
The relative vertical and horizontal accelerations relationships are respectively given by

$$a_v = \tan\theta \, a_{rh} \qquad (5.2)$$

and

$$a_h = a_{rh} + A_g \qquad (5.3)$$

When the angle θ is sufficiently small, say,

$$\theta < 5^0 \qquad (5.4)$$

and let the friction coefficient μ be less than 0.2:

$$\mu < 0.2 \qquad (5.5)$$

in this case,

$$a_h \approx \frac{\sin\theta - \mu\cos\theta}{\cos\theta + \mu\sin\theta} \, g \qquad (5.6)$$

Here, we assume

$$\frac{\sin\theta + \mu\cos\theta}{\cos\theta - \mu\sin\theta}\,\tan\theta \approx 0 \qquad (5.7)$$

Because the quantities θ, μ and g are all constant, the horizontal absolute acceleration is a constant. Note that the ground acceleration, A_g, does not appear in equation (5.6) [Lee et al 2007]. In other words, *the amplitude of the acceleration of the superstructure will be constant*. The first objective of having a constant and low amplitude acceleration of the superstructure thus may be achieved.

Next, if the friction is sufficiently small,

$$\mu << \theta$$

then,

$$a_h \approx \theta\,g \qquad (5.8)$$

The rotation friction coefficient of the rolling motion will only be a fraction of one percent. However, with θ less than 5^0, the angle will be several percent (unit in radians). That is, θ will be about ten times larger than μ. The condition $\mu << \theta$ is then satisfied.

Next, the vertical acceleration can be given as

$$a_v \approx -\,A_g\,\tan\theta \qquad (5.9)$$

Since $\tan\theta \approx \theta$ is for very small angles, the vertical acceleration due to the horizontal ground excitation A_g is very small and can be shown quantitatively that it is negligible [Ou et al 2009].

5.2 Design parameters

The major design parameters for the roller isolation bearing are listed as follows:

Maximum vertical load per bearing: P_r [kips];

Maximum permanent load: L_{pm} [kips]

Lateral force (use the shear pins controlled the lateral force): $0.12L_{pm}$ [kips]

Roller diameter D_r and length l_r:

$$l_r D_r \geq c.P_r \frac{E_s}{8\sigma_y^2}\left[\text{in}^2\right] \qquad (5.10)$$

where

σ_y = specified minimum yield strength of the weakest material at the contact surface

E_s = Young's modulus for material

P_r = load asymmetrical coefficient

c =1 for single direction rolling bearing

c = 0.7 for double direction rolling bearing

Fig. 5.2 shows the configuration of a prototype roller bearing assembly which was manufactured for laboratory studies. Details on the performance and design of roller isolation bearings may be found in publications by the authors and their colleagues that are given in the references.

5.3 Roller bearing implementation

With the support of a Federal Highway Administration grant, the new roller isolation bearing has been installed in an actual bridge to observe the constructability and other related issues in Rhode Island. As of August 2011, the installation is completed and the bridge is open to traffic. Certain monitoring systems are installed so that in time the performance of the roller isolation bearings under ambient live loads can be evaluated. Figure 5.3 contains a number of the New Street Bridge in RI which is the first bridge in the US implemented with the new roller bearings.
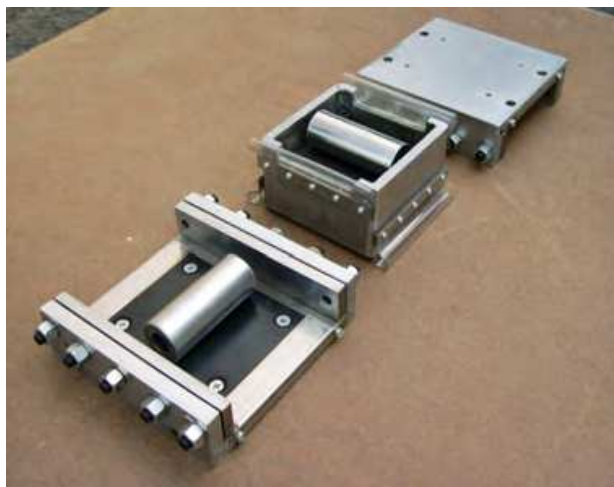
Fig. 5.2. Roller Bearing Assembly

Two Span Bridge Rehabilitation   Roller Isolation Bearing   Installation at Completion

Fig. 5.3. Bridge Rehabilitation in Rhode Island

6. Summary

Although seismic isolation is considered to be a relatively matured technology, there are several issues need to be further explored. The main concern is that in general, the targeted acceleration reduction and the bearing displacement are independent parameters. That is, giving one does not automatically define the other. While for most available isolation systems today, the design practice has been based on the assumption that they are dependent parameters. For this assumption works for many cases, it does not yield adequate design for special situations that can exist. Therefore, principles and approaches to deal with these two independent parameters are needed.

This chapter first discussed several design issues of seismic isolation followed by an explanation of the cases where current design approaches may introduce large errors. Certain key parameters for isolation design are discussed and some research needs are identified. The references provided are selected representative publications by many contributors. No intention was given in this chapter to provide a careful literature review on the subject of seismic isolation.

The main control parameter of the seismic induced vibration is the natural period or effective period of the isolation system. To reduce the acceleration, longer period is needed. However, the longer the period is the larger displacement will be resulted. Thus, isolation design is viewed from the perspective of compromising between acceleration reduction and displacement tolerance.

The second important parameter is the effective damping ratio, because displacement can only be regulated by damping. The issue becomes complicated because adding damping will affect the acceleration reduction.

A base-isolated structure is typically a combination of civil engineering structure with mechanical engineering devices. The former is often designed with sufficient safety redundancy. However, the isolation devices are "precision" mechanical parts that do not have large tolerance of displacement uncertainty. By using the concept of probability based design, the safety margin for base isolation systems may be established with more confidence.

This chapter emphasizes the importance of a design window to consider the demand of acceleration and the displacement. Since large displacement may induce many engineering problems, such as large artificial P-Δ effect, etc. the displacement has to be carefully regulated or controlled. This will narrow the available design window. In some cases, no window is available for a reasonable design of base isolation system, suggesting that for such a case it is not effective to use isolation bearings.

A new type of isolation bearing is briefly explained, which promises to deliver an optimally compromised acceleration reduction and displacement control through addition of damping.

7. Acknowledgement

8. References

AASHTO (2010). *Guide Specifications for Seismic Isolation Design*. Interim 2000. Washington, D.C.

ASCE/SEI standard 41-06 (2007). *Seismic Rehabilitation of Existing Buildings*, American Society of Civil Engineers.

ASCE/SEI standard 7-10 (2010). *Minimum Design Loads of Buildings and Other Structures*, American Society of Civil Engineers.

ATC (1995). *Structural Response Modification Factors*, Report No. ATC-19, Applied Technology Council, Redwood City, California.

Austin, M.A., Lin, W.J. (2004). Energy Balance Assessment of Base-Isolated Structures. *J. Engineering Mechanics*, 130(3), pp. 347-358

Buckle, I., Constantinou, M., Dicleli, M. and Ghasemi, H. (2006). *Seismic Isolation of Highway Bridges*, Special Report MCEER-06-SP07, University at buffalo, The State University of New York.

Buckle, I.G. and Mayes, R.L. (1990). Seismic Isolation: History, Application, and Performance – A World View, *Earthquake Spectra*, 6(2), pp. 161-201.

Christopoulos, C. and Filiatrault, A. (2006). *Principles of Supplemental Damping and Seismic Isolation*. University Institute for Advanced Study (IUSS) Press, University of Pavia, Italy.

Clark, P. W., Whittaker, A. S., Aiken, L. D. and Egan, J. A. (1993). Performance Considerations for Isolation Systems in Regions of High Seismicity, *Proceedings of ATC-17-1 Seminar on Seismic Isolation, Passive Energy Dissipation, and Active Control*, San Francisco, CA, March 11-12, pp. 29-40.

Clough, R. and Penzien, J. (2003). *Dynamics of Structures*. 3rd Ed. Computers and Structures, Inc.

Constantinou, M.C., Caccese, J. and Harris, H.G. (1987). Frictional Characteristics of Teflon-Steel Interfaces under Dynamic Conditions, *Earthquake Engineering and Structural Dynamics*, 15, pp. 751-759.

Constantinou, M.C., Mokha, A.S. and Reinhorn, A.M. (1990). Teflon Bearings in Base Isolation. Part 2: Modeling. *Journal of Structural Engineering*, ASCE, 116(2), pp. 455-474

Constantinou, M.C. (2001). New Developments in the Field of Seismic Isolation, *Proceedings of 2001 Structures Congress*, ASCE, Washington, DC.

European Committee for Standardization (2000). *Structural Bearings*, European Standard EN 1337-1, Brussels.

Fenz, D.M. and Constantinou, M.C. (2006). Behavior of the Double Concave Friction Pendulum Bearing, *Earthquake Engineering and Structural Dynamics*, Vol. 35, No. 11, pp. 1403-1424.

Fenz, D.M. and Constantinou, M.C. (2008). Spherical Sliding Isolation Bearings with Adaptive Behavior: Theory, *Earthquake Engineering and Structural Dynamics*, Vol. 37, No. 2, pp. 163-183.

Fenz, D.M. and Constantinou, M.C. (2008). Spherical Sliding Isolation Bearings with Adaptive Behavior: *Experimental Verification, Earthquake Engineering and Structural Vibration*, Vol. 37, No.2, pp. 185-205.

Hall, J.F., Heaton, T.H., Halling, M.W. and Wald, D.W.J. (1995). Near-Source Ground Motion and Its Effects on Flexible Buildings, *Earthquake Spectra*, 11(4), pp. 569-605

Hall, J.F. and Ryan, K.L. (2000). Isolated Buildings and the 1997 UBC Near-Source Factors, *Earthquake Spectra*, 16(2), pp. 393-411

Inaudi, J.A. and Kelly, J.M. (1993). Optimum Damping in Linear Isolation Systems, *Earthquake Engineering and Structural Dynamics*, 22, pp. 583-598

International Code Council (2000). *International Building Code*, Falls Church, Virginia.

Kelly, J.M. (1986). Aseismic Base Isolation: A Review and Bibliography, *Soil Dynamics and Earthquake Engineering*, 5, 202-216

Kelly, J.M. (1993). State-of-the-Art and State-of-the-Practice in Base Isolation, *Proceedings of ATC-17-1 Seminar on Seismic Isolation, Passive Energy Dissipation, and Active Control*, San Francisco, California, pp.9-28

Kelly, J.M. (1997). *Earthquake Design with Rubber*, Springer-Verlag, Inc.

Kelly, J.M. (1999). The Role of Damping in Seismic Isolation, *Earthquake Engineering and Structural Dynamics*, 28, pp. 3-20.

Kelly, J.M. (1999). The Current State of Base Isolation in United States, *Proceedings of the 2nd World Conference on Structural Control*, Kyoto, Japan, 1, 1043-1052

Kelly, J.M. (2004), Chapter 11, *Seismic Isolation, in Earthquake Engineering*, Borzognia & Bertero (eds), CRC Press LLC.

Komodromos, P.I. (2000). *Seismic Isolation for Earthquake-Resistant Structures*, Southampton, UK : WIT Press

Lee, G.C., Ou Y.-C, Liang Z., Niu T., Song J. (2007). *Principles and Performance of Roller Seismic Isolation Bearings for Highway Bridges*, MCEER Technical Report MCEER-07-0019, December 2007.

Lee, G.C., Ou, Y.-C., Niu, T., Song, J., and Liang, Z. (2010). Characterization of a Roller Seismic Isolation Bearing with Supplemental Energy Dissipation for Highway Bridges, *Journal of Structural Engineering*, ASCE, 136(5), 502-510, May 2010.

Liang, Z. and Lee, G. C. (1991). *Damping of structures, Part 1, Theory of complex Damping*. Technical Report NCEER-91-0004, State University of New York at Buffalo.

Liang, Z., Lee, G. C., Dargush, G. and Song, J. W. (2012*). Structural Damping: Applications in Seismic Response Modification*. CRC Press, 2012.

Lin, T.W., Hone, C.C. (1993). Base Isolation by Free Rolling Rods under Basement. *Earthquake Engineering and Structural Dynamics*, 22, pp. 261-273.

Mosqueda, G., Whittaker, A.S. and Fenves, G.L. (2004). Characterization and Modeling of Friction Pendulum Bearings Subjected to Multiple Components of Excitation. *Journal of Structural Engineering*, 130(3), pp. 433-442.

Mostaghel, N. and Khodaverdian, M. (1987). Dynamics of Resilient-Friction Base Isolator (R-FBI), *Earthquake Engineering and Structural Dynamics,* 11, pp. 729-748.

Naeim, F. and Kelly, J.M. (1999*). Design of Seismic Isolation Structures from Theory to Practice*, John Wiley & Sons Inc.

Nowak, A. S. and Collins, K. R. (2000) *Reliability of Structures* McGraw Hill

Ou, Y.-C., Song, J., and Lee, G.C. (2010). A parametric study of seismic behavior of roller seismic isolation bearings for highway bridges. *Earthquake Engineering and Structural Dynamics,* 39(5), 541-559,April 2010.

Robinson, W.H. (1982). Lead-Rubber Hysteretic Bearings Suitable for Protecting Structures During Earthquakes, *Earthquake Engineering and Structural Dynamics*, 10, pp. 593-604.

Roussis, P.C. and Constantinou, M.C. (2006). Uplift-Restraining Friction Pendulum Seismic Isolation System, *Earthquake Engineering and Structural Dynamics*, Vol. 35, No. 5, April 2006, pp. 577-593.

Skinner, R.I., Robinson, W.H. and McVerry, G.H. (1993). An Introduction to Seismic Isolation, John Wiley & Sons Ltd.

Soong, T.T. and Dargush, G. F. (1997) *Passive Dissipation Systems in Structural Engineering* John Wiley & Sons, New York,

Structural Engineers Association of Northern California (SEAONC) (1986). *Tentative Seismic Isolation Design Requirements*, Yellow Book.

Takewaki, I. (2009) *Building Control with passive Dampers, Optimal Performance-based Design for Earthquakes,* ohn Wiley &

Thompson, A.C.T., Whittaker, A.S., Fenves, G.L. and Mahin, S.A. (2000). Property Modification Factors for Elastomeric Seismic Isolation Bearings, *Proc. 12th World Conference on Earthquake Engineering*, New Zealand.

Tsopelas, P. and Constantinou, M.C. (1997). Study of Eiastoplastic Bridge Seismic Isolation System, *Journal of Structural Engineering,* Vol. 123, No.4, pp. 489-498.

Tsopelas, P., Constantinou, M.C., Kim, Y-S., and Okamoto, S. (1997). Experimental Study of FPS System in Bridge Seismic Isolation. *Structural Engineering and Structural Dynamics*, Vol. 25, No. 1, pp. 65-78.

Wang, J. (2005). *Seismic Isolation Analysis of a Roller Bearing Isolation System*, Ph.D. Dissertation, University at Buffalo, State University of New York, Buffalo, NY, July 2005.

Whittaker, A.S., Constantinou, M.C., and Tsopelas, P. (1998). Displacement Estimates For Performance-Based Seismic Design, *Journal of Structural Engineering*, Vol. 124, No.8, pp. 905-912.

Zayas, V.A., Low, S.S. and Mahin, S.A. (1990). A Simple Pendulum Technique for Achieving Seismic Isolation, *Earthquake Spectra*, 6, pp. 317-334

Zhou, Q., Lu, X.L., Wang, Q.M., Feng, D.G., Yao, Q.F. (1998). Dynamic Analysis on Structures Base-isolated by a Ball System with Restoring Property. *Earthquake Engineering and Structural Dynamics*, 27, pp. 773-791.
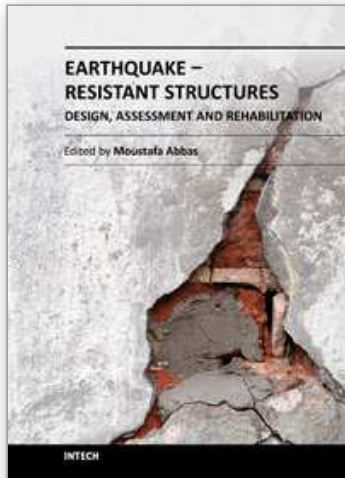
Earthquake-Resistant Structures - Design, Assessment and Rehabilitation

Edited by Prof. Abbas Moustafa

ISBN 978-953-51-0123-9

Hard cover, 524 pages

Publisher InTech

Published online 29, February, 2012

Published in print edition February, 2012

This book deals with earthquake-resistant structures, such as, buildings, bridges and liquid storage tanks. It contains twenty chapters covering several interesting research topics written by researchers and experts in the field of earthquake engineering. The book covers seismic-resistance design of masonry and reinforced concrete structures to be constructed as well as safety assessment, strengthening and rehabilitation of existing structures against earthquake loads. It also includes three chapters on electromagnetic sensing techniques for health assessment of structures, post earthquake assessment of steel buildings in fire environment and response of underground pipes to blast loads. The book provides the state-of-the-art on recent progress in earthquake-resistant structures. It should be useful to graduate students, researchers and practicing structural engineers.

How to reference

In order to correctly reference this scholarly work, feel free to copy and paste the following:

George C. Lee and Zach Liang (2012). Design Principles of Seismic Isolation, Earthquake-Resistant Structures - Design, Assessment and Rehabilitation, Prof. Abbas Moustafa (Ed.), ISBN: 978-953-51-0123-9, InTech, Available from: http://www.intechopen.com/books/earthquake-resistant-structures-design-assessment-and-rehabilitation/design-principles-of-seismic-isolation

INTECH

open science | open minds